Salt Intrusion into Fresh-Water Aquifers

HAROLD R. HENRY

U. S. Geological Survey and Michigan State University
East Lansing, Michigan

Abstract—In a coastal aquifer a steady flow of fresh water toward the sea can limit the encroachment of the salt water into the aquifer. This action is treated on the assumptions that the flow is steady and two-dimensional, that the salt and fresh water are immiscible, and that there is no fingering. Theoretical equations for the shape and location of the interface and for the boundary velocities are derived for several sets of boundary conditions.

The uncertainty of the location of the interface is circumvented by use of a hodograph plane. In addition, a complex potential is employed and related to the hodograph by conformal mapping.

Certain boundary conditions represent inversions of gravity seepage through dams for which solutions already exist. Numerical computations are also presented for a semi-infinite aquifer having a vertical seepage face and one having a horizontal seepage face.

Introduction—The location of the interface between the salt and fresh water in a coastal aquifer is of obvious interest in the practical use of ground water. The seaward flow of fresh water in the aquifer is necessary to keep salt water from contaminating the aquifer. As a first approximation to this action, exact solutions have been obtained for several boundary conditions, on the assumption that the salt and fresh water are immiscible and that there is no fingering and no tidal action. The effects of diffusion and tidal action result in a 'zone of diffusion' which will be investigated as a continuation of the present study.

The configurations analyzed are shown in Figures 1 and 6. In Figure 1 the seepage face AB is vertical, and in Figure 6 it is horizontal. In each case the problem is solved first for a finite aquifer as shown. The equations are subsequently modified to solve the cases where the aquifer extends to infinity to the left. Another limiting case which is treated is that of an aquifer that is infinite in extent to the left and infinite in depth also.

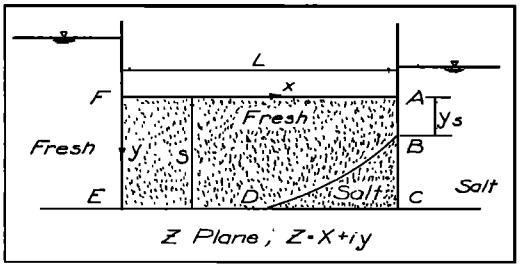

FIG. 1—Case I, horizontal confined aquifer with vertical outflow face.

Notation—The following symbols are used.

A, B, C, D, E, F	points on the boundary of the aquifer
a, b, c, d, e	coordinates of points in the complex plane
$f(z)$	complex velocity potential $= \phi + i\psi$
$f'(z)$	first derivative of f with respect to z
$f''(z)$	second derivative of f with respect to z
h	piezometric head, in feet of fresh water
i	$\sqrt{-1}$
J	the elliptic modular function
K	complete elliptic integral of first kind
K'	complete elliptic integral of first kind, with complementary modulus
k	modulus of elliptic integral
$\bar{k}$	permeability of aquifer
k'	product of permeability and buoyancy $= \bar{k}(\gamma_s - \gamma_0)/\gamma_0$
L	length of aquifer
Q	discharge per unit width
q	complex velocity $= u + iv$
$\bar{q}$	conjugate complex velocity $= u - iv$
q_1, q_2	transformations of the hodograph
S	depth of aquifer
λ, w, t	complex variables

u velocity in x direction
v velocity in y direction
x horizontal coordinate
y vertical coordinate measured downward
z complex variable
α the integral, $-\frac{3}{2\pi}\int_0^1 \frac{\beta(t)}{t-\lambda}\,dt$
β central angle in hodograph plane
γ_s specific weight of salt water
γ_0 specific weight of fresh water
ϕ velocity potential
ψ stream function
$\tau + i\theta$ the auxiliary variable

Governing Equations and Boundary Conditions—The use of Darcy's law for a homogenous two-dimensional aquifer,

$$u = -\partial\phi/\partial x, \qquad v = -\partial\phi/\partial y \tag{1}$$

in the continuity equation,

$$\partial u/\partial x + \partial v/\partial y = 0 \tag{2}$$

yields Laplace's equation for ϕ:

$$\nabla^2\phi = 0 \tag{3}$$

A stream function ψ orthogonal to ϕ can be defined by the Cauchy-Riemann equations and a complex velocity potential $f(z)$ written as

$$f(z) = \phi + i\psi \tag{4}$$

The conjugate of the complex velocity is defined by

$$\bar{q} = u - iv = -f'(z) \tag{5}$$

The variation of ϕ along the interface of salt and fresh water and along the seepage surface is controlled by the pressure in the salt water, which is assumed to be at rest. Thus along AB and BD in Figures 1 and 6

$$\phi = \phi_0 + k'y \tag{6}$$

where ϕ_0 is constant and y is measured downward. Differentiation of ϕ with respect to the distance r along the surface of seepage AB yields

$$-\partial\phi/\partial r = u_r = u\cos\alpha + v\sin\alpha \tag{7}$$

where α is the angle between the seepage surface and the horizontal; α is $\pi/2$ in Figure 1 and zero in Figure 6. Substitution of (6) into (7) yields

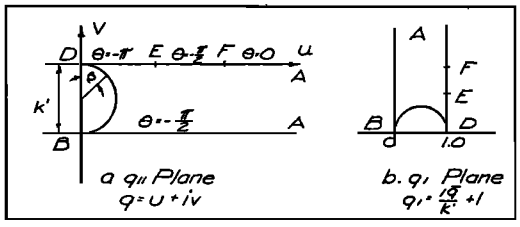

FIG. 2—Hodograph for case I.

$$k'\sin\alpha + u\cos\alpha + v\sin\alpha = 0 \tag{8}$$

This is the equation of the line in the hodograph plane (u,v) representing the velocity on AB. (See Figs. 2a and 7a).

Differentiation of (6) with respect to distance s along the interface BD yields

$$\partial\phi/\partial s = -k'(\partial y/\partial s) \tag{9}$$

Since the interface is a streamline, $\partial\phi/\partial s$ is the total velocity $(u^2 + v^2)^{1/2}$. Multiplying (9) by this factor gives

$$u^2 + v^2 + k'v = 0 \tag{10}$$

Equation (10) is a circle in the hodograph or q plane.

The hodograph for a flow boundary that is a straight line of constant potential is a straight line passing through the origin and perpendicular to the real boundary. For a straight-flow boundary that is a streamline, the hodograph line passes through the origin parallel to the real boundary.

The problem is solved in the following manner. First, the velocities on the boundaries of the flow system are mapped on the hodograph plane. In general u and v or a relationship between u and v is required for every point on the boundary. Next, the complex potential for the boundaries of the flow system is determined. Now if the hodograph diagram is transformed into the f diagram by some function, this function can be substituted directly into (5), which can subsequently be integrated to obtain the solution. It is not always feasible to transform f directly into q, and it may be convenient to employ auxiliary planes to effect the transformation in several steps. Further, if f is not known

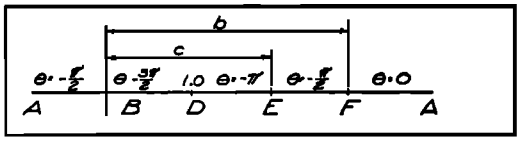

FIG. 3—The λ plane; $\lambda(q_1) = J(1 - 1/q_1)$.

along some portion of the boundary, an auxiliary function of f may be introduced to make the problem tractable.

Case I. Vertical outflow face—The area *ABDEF* (Fig. 1) is saturated with fresh water. The area *BCD* contains salt water at rest. The accompanying hodograph is shown in Figure 2a. The q_1 plane (Fig. 2b) is a modified hodograph defined by

$$q_1 = (i/k')\bar{q} + 1 \tag{11}$$

The zero-angle triangle, with the semicircular side, in the q_1 plane (Fig. 2b), can be transformed into the upper half-plane shown in Figure 3 by use of the elliptic modular function $J(q_2)$ as defined by *Nehari* [1952] and by *Jahnke and Emde* [1945]. Using

$$q_2 = 1 - 1/q_1 \tag{12}$$

we have

$$\lambda(q_1) = J(q_2) \tag{13a}$$

The values of λ corresponding to the flow boundaries can be computed by using the inverse of the elliptic modular function:

$$1 - \frac{1}{q_1} = \frac{iK'(\lambda)}{K(\lambda)} \equiv i\frac{K'}{K}(\lambda) \tag{13b}$$

Values of K'/K for λ real and between zero and unity are given by *Hayashi* [1930]. Thus, within this range, arbitrary values of λ may be substituted into (13b) and corresponding values of q computed. For other ranges of λ simple linear transformations are required to permit use of the tabular values.

For $-\infty < \lambda \leq 0$ one may use

$$1/(1 - \lambda) = J(q_1) \tag{14a}$$

$$q_1 = i\frac{K'}{K}\left(\frac{1}{1 - \lambda}\right) \tag{14b}$$

for $1 \leq \lambda < \infty$ one may use

$$1/\lambda = J(q_1 - 1) \tag{15a}$$

$$q_1 - 1 = \frac{iK'}{K}\left(\frac{1}{\lambda}\right) \tag{15b}$$

Equations 13a or b, 14a or b, and 15a or b may be considered alternate forms of the same transformation between q_1 and λ.

To complete the solution of the problem, it is necessary to express the complex potential f, or some function of f, in terms of $\bar{q}$ so that equation (5) may be integrated. Because the distribution of ψ on AB in Figure 1 is unknown, the method of *Hamel* [1934] is followed. Use is made of the function

$$\tau + i\theta = -\ln[-f''(z)] \tag{16}$$

in which

$$-f''(z) = \frac{du - idv}{dx + idy} \tag{17}$$

and $(-\theta)$ is the argument of $-f''(z)$. From (17) and the hodograph it follows that

$$\theta_{AB} = -\pi/2; \quad \theta_{BD} = -3\beta/2$$
$$\theta_{DE} = -\pi; \quad \theta_{EF} = -\pi/2; \quad \theta_{FA} = 0 \tag{18}$$

The angle β in the second of equations (18) is indicated in the hodograph in Figure 2.

Referring to Figure 3, we see that the values of θ are known at all points of the real axis of the λ plane. Values of θ may then be obtained for all points of the upper half plane by a Fourier integral solution. Subsequently values of τ are obtained by integrating the Cauchy-Riemann equations for τ and θ. *Muskat* [1937] gives details of this procedure which leads to the generalized Poisson formula:

$$\tau + i\theta = \tau_0 + \frac{1}{\pi}\int_{-\infty}^{\infty} \frac{\theta(t)(\lambda t + 1)\,dt}{(t - \lambda)(1 + t^2)} \tag{19}$$

where τ_0 is an arbitrary constant.

Evaluating the integral in (19) and applying the results in (16) yields, after solving for $-f''$,

$$-f'' = \frac{-\sqrt{\lambda(c - \lambda)(b - \lambda)}}{1 - \lambda} \cdot \exp\left(-\tau_0 + \frac{3}{2\pi}\int_0^1 \frac{\beta(t)}{t - \lambda}\,dt\right) \tag{20}$$

where b and c are the coordinates of points E and F respectively in the λ plane. Differentia-

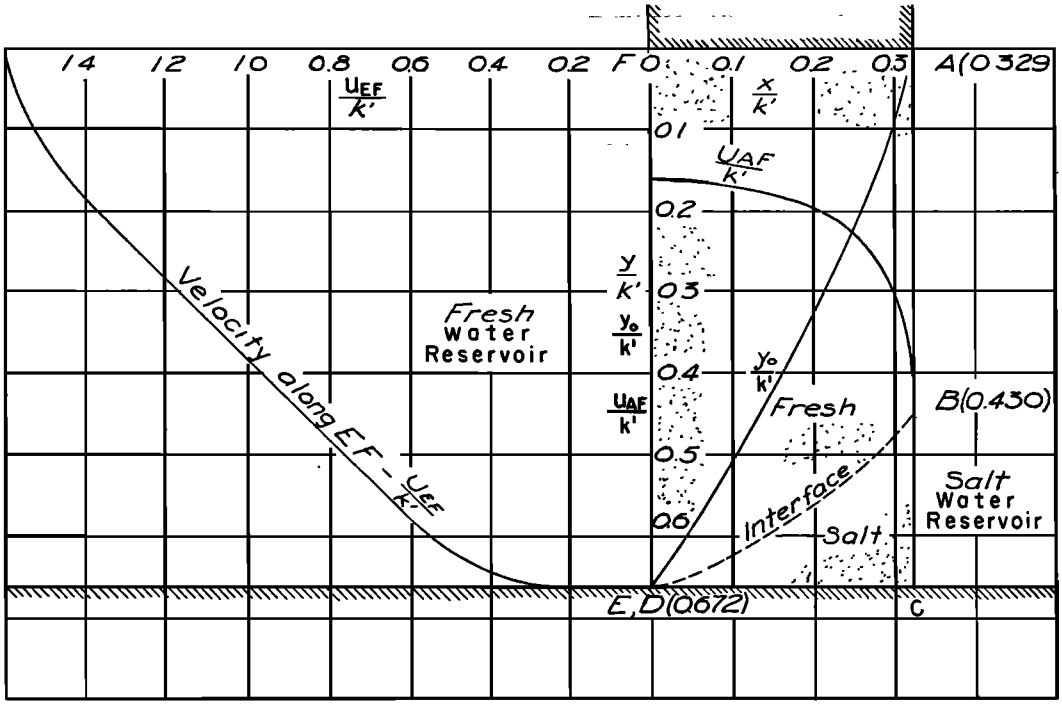

FIG. 4—Salt intrusion under a short sand formation (An inversion of Muskat's case III; curves are identical to Muskat's).

tion of (5) and substitution into (20) gives, after solving for z,

$$z = c_1 \int e^{\tau + i\theta}\, d\bar{q} + C_2 \qquad (21)$$

where

$$e^{\tau} = \frac{1 - \lambda}{\sqrt{\lambda(c - \lambda)(b - \lambda)}}\, e^{\alpha} \qquad (22)$$

and

$$e^{\alpha} = \exp\left(-\frac{3}{2\pi}\int_0^1 \frac{\beta(t)}{t - \lambda}\, dt\right) \qquad (23)$$

Hamel and Gunther [1935] and *Muskat* [1935] give tabulated and graphical values of e^{α} as a function of λ. Thus, the velocities at the boundaries of the flow and the location of the interface may be computed by substituting arbitrary real values of λ into the proper equation, (13), (14), or (15), and by subsequent graphical or numerical integration of (21).

If the relative positions of the levels of the fresh water and the salt water in Figure 1 are such that point D coincides with E—that is, the interface reaches to the upstream reservoir—then $\phi_E = \phi_D$ and

$$e^{\tau} = \sqrt{\frac{1 - \lambda}{\lambda(b - \lambda)}}\, e^{\alpha} \qquad (24)$$

This case is mathematically identical with the case of seepage through a rectangular dam with no tailwater in which the permeability k has been replaced by k'. *Muskat* [1935] gives numerical solutions for the discharge Q and the height of seepage surfaces AB for four such cases. He plots computed boundary velocities for two cases and also draws in the free surface without calculation, following the general features of a previous case with tailwater computed by *Hamel and Gunther* [1935]. Muskat's curves have been inverted and relabeled to fit the present application, as shown in Figures 4 and 5.

When the aquifer extends an infinite distance to the left in Figure 1 the point E in the hodograph coincides with point F and e^{τ} becomes

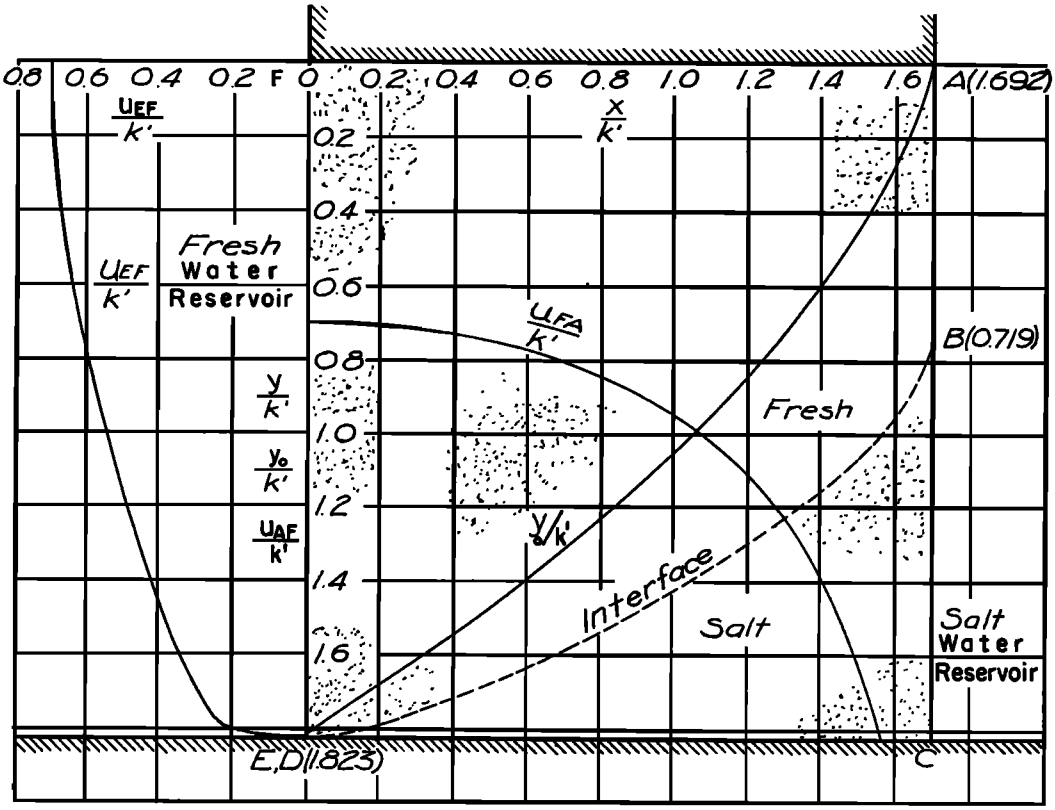

FIG. 5—Salt intrusion under a short sand formation (An inversion of Muskat's case VI; curves are identical to Muskat's).

$$e^{\tau} = \frac{1 - \lambda}{(c - \lambda)\sqrt{\lambda}} e^{\alpha} \qquad (25)$$

Moreover, if the aquifer also extends an infinite distance downward, the hodograph points D, E, and F coincide and e^{τ} becomes

$$e^{\tau} = (1/\sqrt{\lambda})e^{\alpha} \qquad (26)$$

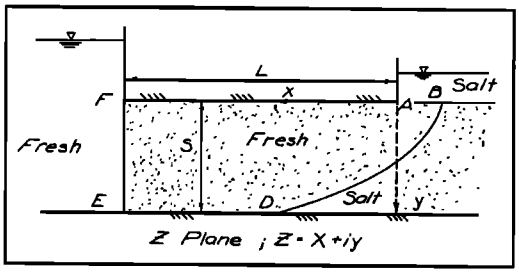

FIG. 6—Case II, horizontal confined aquifer with horizontal outflow face.

The numerical solution for this case is given in the last section of this paper.

Case II. Horizontal outflow face—Figure 6 represents a flow in which the seepage face AB is horizontal. (*Polubarinova-Kochina* [1940] discusses the unsteady characteristics of a similar case.) The hodograph or q plane for the present case is shown in Figure 7a and a transformed hodograph (q_1 plane) is shown in 7b. By use of the Schwarz-Christoffel theorem, the semi-infinite strip of the q_1 plane may be transformed to the upper half of the t plane of Figure 8 by

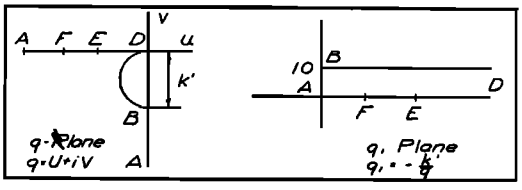

FIG. 7—Hodograph for case II.

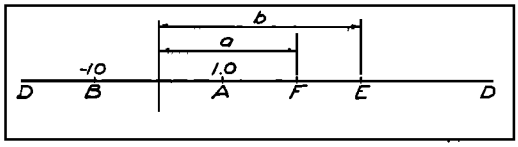

FIG. 8—The t plane; $t = \cosh \pi q_1 = \cosh - \pi k'/q$.

$$t = \cosh \pi q_1 = \cosh (- \pi k'/\bar{q}) \quad (27a)$$

or inversely

$$\bar{q} = (-\pi k')/(\cosh^{-1} t) \quad (27b)$$

In the complex potential plane f the boundaries of the flow form the rectangle shown in Figure 9, where the potential along the seepage

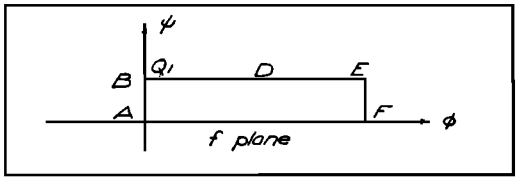

FIG. 9—Complex potential for case II.

face AB is taken as zero. The method of Hamel which introduces the function $\tau + i\,\theta$ defined by (16) could be employed in this case also with a result similar to equation (20). However, it would be tedious to compute the exponential factor similar to e^{α}. This difficulty is obviated by using a more direct method of mapping the rectangle in the f plane into the infinite strip of the q_1 plane by transforming each into the identical half-plane. This is accomplished by first mapping f into the upper half w plane of Figure 10, using the Schwarz-Christoffel theorem:

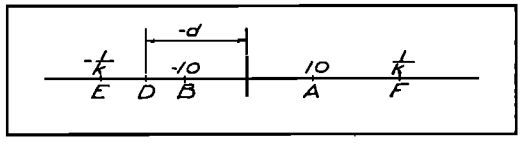

FIG. 10—w plane; $w = sn\ [(\text{if } 2/Q + 1)K]$.

$$w = sn[if(2/Q) + 1]K \quad (28a)$$

or inversely

$$f = \frac{Q}{2i}\left(\frac{sn^{-1} w}{K} - 1\right) \quad (28b)$$

where

$$sn^{-1} w = \int_0^w \frac{dw}{\sqrt{(1 - w^2)(1 - k^2 w^2)}} \quad (28c)$$

and

$$K = sn^{-1}(1, k)$$

The t plane of Figure 3 can be mapped into the w plane by the linear transformation

$$w = \frac{td - 1}{d - t} \quad (29)$$

where $-d$ is the coordinate of point D in the w plane. The relation between the coordinates a and b of the t plane and the values d and k of the w plane are found by substitution into (29)

$$a = \frac{d + k}{kd + 1} \quad (30)$$

$$b = \frac{k - d}{kd - 1} \quad (31)$$

Thus the problem is solved in principle, since $\bar{q}$ is expressed parametrically in terms of f through (27b), (28b), and (29), and in principle (5) can be integrated to give

$$z = \int \frac{-df}{\bar{q}} + \text{const.} \quad (32)$$

The numerical solution of a particular case requires given values of either a and b or d and k. Assuming either pair of values corresponds in effect to assigning values to the two dimensionless quantities $Q/k'S$ and L/S, where S is the vertical thickness of the aquifer and L is its length.

For the case of a horizontal strip of aquifer semi-infinite in length (Fig. 6), the points E and F are at an infinite distance to the left, the two corresponding points in the hodograph are coincident, and in the t plane, $a = b$. Also in Figure 9, E and F would be at infinity to the right. In the w plane this requires that $k = 0$ and that the points E and F be at infinity. Thus equation (28b) transforming the w plane into the f plane degenerates into

$$f = \frac{Q}{\pi} \cosh^{-1} w \quad (33)$$

The relation between the w and t planes is still expressed by (29), and (30) and (31) degenerate into $a = b = d$. Numerically, a particular case is determined by assigning a value to either a or d which in principle corresponds to a certain value of the ratio $Q/k'S$.

Finally, if in Figure 6, in addition to L becoming infinite, the vertical thickness S becomes infinite also, the points D, E, and F will coincide in the hodograph. Then, upon division by Q, the f plane becomes identical to the q_1 plane, yielding

$$f/Q = -k'/\bar{q} \tag{34}$$

For this case, (32) can be integrated to yield

$$z = f^2/2k'Q \tag{35}$$

This is mathematically identical with a seepage problem solved by *Kozeny* [1953] for a free-surface flow in a semi-infinite aquifer draining downward through a horizontal-outflow face with k' substituted for $\bar{k}$. This correspondence between the Kozeny solution and the salt-intrusion problem for the semi-infinite aquifer has been noted and utilized by *Glover* [1959].

Computations for the semi-infinite cases I and II—In order to compare the numerical results for horizontal and vertical seepage faces, dimensionless plots are presented for each case. It should be noted that all solutions of the semi-infinite problem, case I, are geometrically similar. This is true also in the semi-infinite space of case II. For case I (18) and (26) are substituted into (21), for which values of $\bar{q}$ are computed from the appropriate equation, (13), (14), or (15). Then (21) is integrated numerically or graphically. Along AB, λ varies from $-\infty$ to zero and the corresponding values of $\bar{q}$ are computed from (14b), which in this case is

$$\frac{u}{k'} = \frac{K'}{K}\left(\frac{1}{1-\lambda}\right) \tag{36}$$

Values of K'/K may be found in *Hayashi's* tables [1930]. Values of e^{α} are taken from *Hamel and Gunther* [1935]. The integration indicated by (21) was performed by the trapezoidal rule up to a value of $u = 2.8$ corresponding to $\lambda = -400$. For larger negative values of λ the analytic approximation introduced by *Hamel* and *Gunther* [1935] was used

$$\frac{d\bar{q}}{k'} \cong \frac{1}{\pi}\frac{d\lambda}{\lambda}; \qquad e^{\alpha} \cong 1 \tag{37}$$

Computed depth y_s of the seepage surface AB is

$$\frac{y_s k'}{Q} = 0.741$$

as shown in Figure 11.

For the interface BD, equation (10) yields

$$\bar{q} = \frac{-\imath k'}{2}(e^{i\beta} - 1) \tag{38}$$

and use of equations (18) and (26) yields

$$\int e^{\tau + i\theta}\, d\bar{q} = \int \frac{k'}{2}\frac{1}{\sqrt{\lambda}} e^{\alpha} e^{-i\beta/2}\, d\beta \tag{39}$$

Solving for the x and y coordinates from equation (21) gives

$$\frac{k'(x - x_B)}{Q} = \frac{1}{2}\int_{\pi}^{\beta} \cos\frac{\beta}{2}\cdot\frac{1}{\sqrt{\lambda}} e^{\alpha}\, d\beta \tag{40a}$$

$$\frac{k'(y - y_B)}{Q} = \frac{1}{2}\int_{\pi}^{\beta} \sin\frac{\beta}{2}\cdot\frac{1}{\sqrt{\lambda}} e^{\alpha}\, d\beta \tag{40b}$$

Values of β corresponding to given values of λ were computed with (13b), which in view of (11) and (38) may be rewritten as

$$\tan\beta/2 = \frac{K'}{K}(\lambda) \tag{41}$$

The integrals of equations (40a) and (40b) were computed by the trapezoidal rule to give the coordinates of the interface, shown by the solid line marked BD in Figure 11.

The piezometric head on the boundary AF is indicated by the line with ordinate $k'y_0/Q$ in Figure 11. The depth y_0 (x) would be the ordinate of the interface if hydrostatic conditions prevailed along vertical sections. This computation requires first the computation of u versus x as shown by the solid curve above AF. The latter proceeds from a graphical integration of (21), by use of (15) for the relation between λ and q_1. The head was subsequently computed by

$$h_x - h_A = y_0\left(\frac{\gamma_s - \gamma_0}{\gamma_0}\right) = \int \frac{u}{\bar{k}}\, dx \tag{42a}$$

$$\frac{k'y_0}{Q} = \int \frac{u}{k'}\, d\left(\frac{xk'}{Q}\right) = \int \frac{u}{k'} e^{\tau}\, \frac{du}{k'} \tag{42b}$$

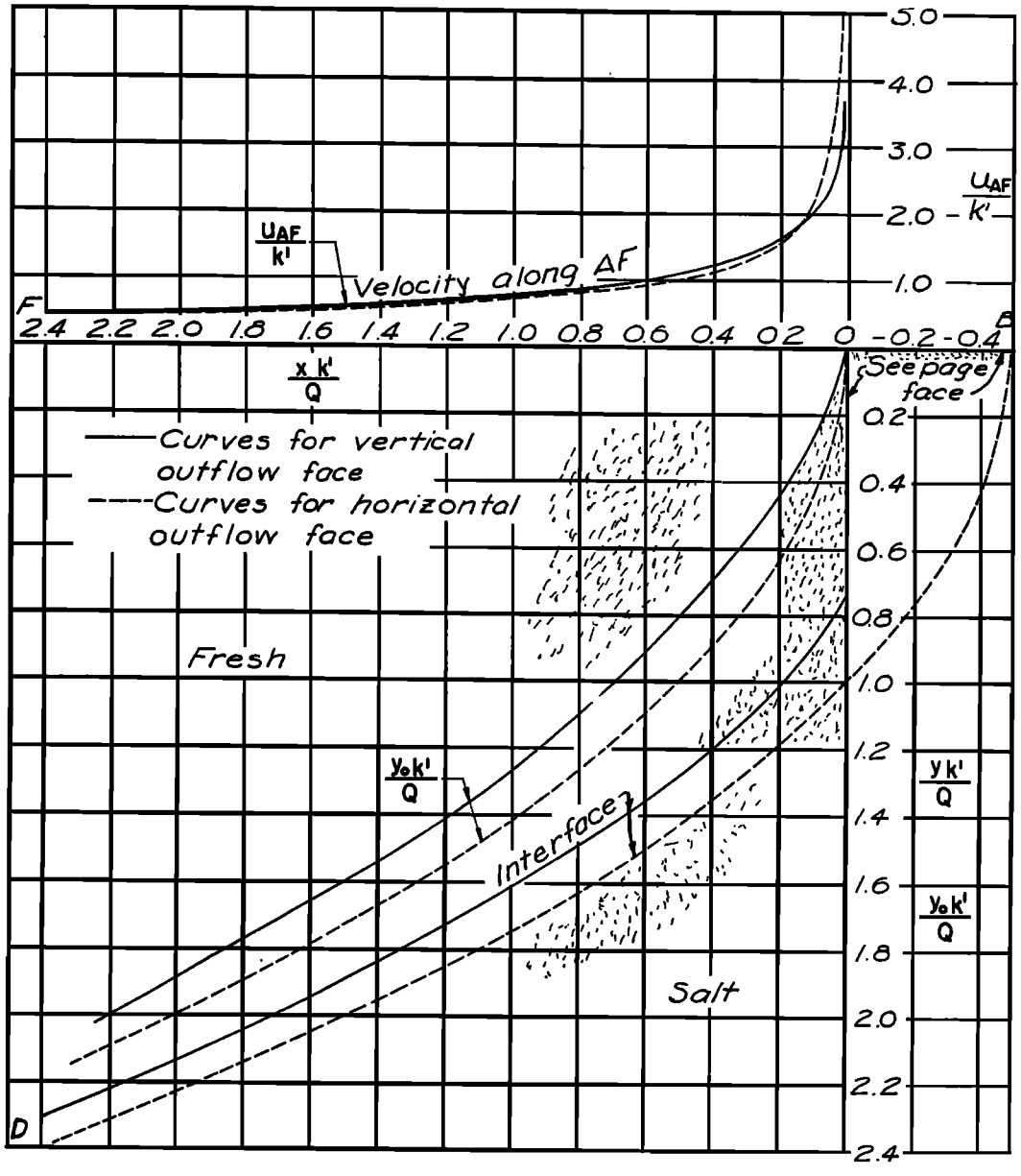

FIG. 11—Numerical solution of the semi-infinite aquifer for cases I and II.

in which h_s represents the head on AF at any abscissa and h_A represents the head at A in feet of fresh water. Equation (42b) was integrated graphically to produce the upper curve for $k'Y_o/Q$ shown in Figure 11.

Computations for case II with a horizontal-outflow face are much simpler. The width of the seepage surface is obtained by substituting $y = 0$, $x = x_s$, $\psi = Q$, and $\phi = 0$ into (35). The result is

$$x_s k'/Q = -\tfrac{1}{2} \qquad (43)$$

The interface is computed by substituting $\psi = Q$ and $\phi = k'y$ into (35).

$$\left(\frac{yk'}{Q}\right)^2 - 2\left(\frac{xk'}{Q}\right) - 1 = 0 \qquad (44)$$

The dashed curve BD in Figure 11 is a plot of (44).

The piezometric head on AF, indicated by y_0, is obtained by substituting $\psi = 0$ and $y = 0$ into (35) and solving for y_0.

$$\frac{y_0 k'}{Q} = \sqrt{2\left(\frac{xk'}{Q}\right)} \qquad (45)$$

The velocity along AF is given by differentiating ϕ.

$$\frac{u}{k'} = -\frac{1}{k'}\frac{\partial \phi}{\partial x} = -\sqrt{\frac{1}{2}\left(\frac{Q}{xk'}\right)} \qquad (46)$$

Equation (46) is plotted in Figure 11.

Conclusions—Theoretical solutions for the salt encroachment problem, assuming salt and fresh water to be immiscible, have been derived for six cases. The two basic cases are shown in Figures 1 and 6. Two special cases occur for aquifers infinite to the left in Figures 1 and 6 and the two final cases are for aquifers of infinite depth.

The numerical results for the infinite-depth aquifers (Fig. 11) represent extreme inclinations of the outflow face and indicate the limits of the location of the interface for intermediate cases.

Additional numerical results for particular cases of aquifers of finite depth and length in which the interface extends just to the upstream edge of the formation are shown in Figures 4 and 5.

In addition to the location of the interface, the numerical results also include distribution of velocities u_{AF} along the upper boundary of the aquifer and, for the finite formations, velocities u_{EF} along the vertical entrance to the aquifer. Also of interest is the location of y_0 when compared with the actual location of the interface. It is again noted that y_0 would give the location of the interface if lines of constant piezometric head were vertical instead of concave toward the sea. For an unconfined aquifer y_0 would be the location of the interface as estimated by the Ghyben-Herzberg principle of balance of pressures and, as can be seen in Figures 4, 5, and 11, this type of estimate usually indicates considerably more encroachment than actually occurs.

The results make available a rational theory which can be compared with field measurements and model tests. In future studies an attempt will be made to superimpose the effects of diffusion to obtain a more realistic representation of field conditions.

Acknowledgments—The writer wishes to thank Richard Skalak of Columbia University for constant encouragement and advice and for reviewing the manuscript. Also, thanks are due Emmett Laursen of Michigan State University for helpful discussions and suggestions. The study was suggested by discussions with R. R. Bennett and H. H. Cooper, Jr. of the U. S. Geological Survey, and their cooperation is gratefully acknowledged.

References

Glover, R. E., The pattern of fresh-water flow in a coastal aquifer, *J. Geophys. Research, 64,* 457–459, 1959.

Hamel, G., Über Grundwasserströmung, *Z. angew. Math. u. Mech., 14,* 130–157, 1934.

Hamel, G., and E. Günther, Numerische Durchrechnung zu der Abhandlung über Grundwasserströmung, *Z. angew. Math. u. Mech., 15,* 255–265, 1935.

Hayashi, K., *Tafeln der Besselschen, Theta, Kugel, und anderer Funktionen,* Springer, Berlin, 125 pp., 1930.

Jahnke, Eugene, and Fritz Emde, *Tables of Functions,* Dover Publications, New York, 304 pp., 1945.

Kozeny, Joseph, *Hydraulik,* Springer, Wien, 588 pp., 1953.

Muskat, Morris, The Seepage of Water through Dams with Vertical Faces, *Physics, 6,* 402–415, 1935.

Muskat, Morris, *The Flow of Homogeneous Fluids through Porous Media,* McGraw-Hill, New York, 763 pp., 1937.

Nehari, Zeev, *Conformal Mapping,* McGraw-Hill, New York, 396 pp., 1952.

Polubarinova-Kochina, P. Y., On the unsteady motion of ground water in two layers of different density (in Russian), *Izvest. Akad. Nauk SSSR, Otdel Tekh. Nauk, No. 6,* 1940.

(Manuscript received July 16, 1959; presented at the Fortieth Annual Meeting, Washington, D. C., May 5, 1959.)